Doppler-Derived Ejection Intraventricular Pressure Gradients Provide a Reliable Assessment of Left Ventricular Systolic Chamber Function

Raquel Yotti, MD; Javier Bermejo, MD, PhD; M. Mar Desco, MD, PhD; J. Carlos Antoranz, PhD; José Luis Rojo-Álvarez, MEng, PhD; Cristina Cortina, MD; Carmen Allué, RDNS; Hugo Rodríguez-Abella, MD; Mar Moreno, MD, PhD; Miguel A. García-Fernández, MD, PhD

Background—Ejection intraventricular pressure gradients are caused by the systolic force developed by the left ventricle (LV). By postprocessing color Doppler M-mode (CDMM) images, we can measure noninvasively the ejection intraventricular pressure difference (EIVPD) between the LV apex and the outflow tract. This study was designed to assess the value of Doppler-derived EIVPDs as noninvasive indices of systolic chamber function.

Methods and Results—CDMM images and pressure-volume (conductance) signals were simultaneously acquired in 9 minipigs undergoing pharmacological interventions and acute ischemia. Inertial, convective, and total EIVPD curves were calculated from CDMM recordings. Peak EIVPD closely correlated with indices of systolic function based on the pressure-volume relationship: peak elastance (within-animal $R=0.98$; between-animals $R=0.99$), preload recruitable stroke work (within-animal $R=0.81$; between-animals $R=0.86$), and peak of the first derivative of pressure corrected for end-diastolic volume (within-animal $R=0.88$; between-animals $R=0.91$). The correlation of peak inertial EIVPD with these indices was also high (all $R>0.75$). Load dependence of EIVPDs was studied in another 5 animals in which consecutive beats obtained during load manipulation were analyzed. During caval occlusion (40% EDV reduction), dP/dt_{max}, ejection fraction, and stroke volume significantly changed, whereas peak EIVPD remained constant. Aortic occlusion (40% peak LV pressure increase) significantly modified dP/dt_{max}, ejection fraction, and stroke volume; a nearly significant trend toward decreasing peak EIVPD was observed ($P=0.06$), whereas inertial EIVPD was unchanged ($P=0.6$). EIVPD beat-to-beat and interobserver variabilities were $2\pm12\%$ and $5\pm11\%$, respectively.

Conclusions—Doppler-derived EIVPDs provide quantitative, reproducible, and relatively load-independent indices of global systolic chamber function that correlate closely with currently available reference methods. **(*Circulation*. 2005; 112:1771-1779.)**

Key Words: hemodynamics ■ systole ■ echocardiography ■ imaging ■ pressure

An accurate evaluation of left ventricular (LV) systolic function in the clinical setting is a persistent challenge. The contractile state of the myocardium is generally assessed indirectly by analysis of systolic chamber function because intrinsic myocardial function is very difficult to measure in vivo.[1] At this chamber integration level, a number of indices have been proposed to account for LV systolic function. Among these, indices based on the pressure-volume relationship are established as the most reliable standards available in vivo because of their sensitivity, accuracy, and load independence.[2,3] However, the need for instantaneous high-fidelity measurements of intraventricular pressure and volume and for acute preload modification maneuvers has prevented their widespread use in clinical practice.

See p 1684

Intraventricular pressure gradients were first measured with micromanometers >50 years ago.[4] Generated by the active force of the contracting ventricle,[5,6] the instantaneous ejection intraventricular pressure difference (EIVPD) between the LV apex and the outflow tract (LVOT) has shown to be related to the inotropic state.[7–9] In the absence of

Received June 16, 2004; revision received February 10, 2005; accepted June 1, 2005.

From the Department of Cardiology (R.Y., J.B., C.C., C.A., M.M., M.A.G.-F.), Unit of Experimental Medicine and Surgery (M.M.D.), and Department of Cardiovascular Surgery (H.R.-A.), Hospital General Universitario Gregorio Marañón, Madrid; Department of Mathematical Physics and Fluids, Facultad de Ciencias, Universidad Nacional de Educación a Distancia, Distancia (J.C.A.); and Department of Signal Theory and Communications, Universidad Carlos III de Madrid, Madrid (J.L.R.-A.), Spain.

Presented in part at the 2004 American Heart Association Scientific Sessions, New Orleans, La, November 7–10, 2004, and published in abstract form (*Circulation*. 2004;110[suppl III]:III-424).

The online-only Data Supplement can be found at http://circ.ahajournals.org/cgi/content/full/112/12/1771/DC1.

Correspondence to Javier Bermejo, MD, PhD, Laboratory of Echocardiography, Department of Cardiology, Hospital General Universitario Gregorio Marañón, Dr Esquerdo 46, 28007 Madrid, Spain. E-mail javbermejo@jet.es

Circulation **is available at http://www.circulationaha.org** **DOI: 10.1161/CIRCULATIONAHA.104.485128**

outflow obstruction, the EIVPD reaches its peak early during systole and is fundamentally caused by impulsive forces. It is worth noting that the diagnostic value of the ventricular impulse was the basis for developing well-established indices of systolic function such as the first time derivative of pressure (dP/dt_{max}) and flow acceleration.[10] Theoretical evidence further supports that peak EIVPD may be a sensitive index of systolic chamber function.[11]

We have recently developed and validated a new method to obtain noninvasive measurements of EIVPDs by postprocessing color Doppler M-mode (CDMM) echocardiograms.[12,13] The present study was designed to study the utility of EIVPD as a noninvasive index of systolic chamber function in vivo with a high-fidelity pressure and conductance instrumentation animal setup. The specific objectives were (1) to correlate Doppler-derived EIVPDs with invasive reference indices of systolic function in a range of inotropic states induced by pharmacological interventions and acute ischemic cardiomyopathy (study 1), (2) to assess the modification of EIVPDs caused by acute load changes (study 2), and (3) to assess the potential error caused by scan line misalignment on the estimation of EIVPDs (study 3).

Methods

Experimental Protocols

Minipigs (60±10 kg) were used for all experiments. Adult animals were selected because their LVOT flow velocity profile closely resembled that of normal adult humans.[14] An open-chest closed-pericardium model was used for study 1 to obtain the highest-quality epicardial echocardiographic sequences for calibrating the conductance volume signal. A closed-chest model was used for study 2 because of the known effects of sternotomy on the load dependence of indices of systolic chamber function.[15] The study protocol was approved by the local Institutional Animal Care Committee.

Animals were preanesthetized with ketamine and xylazine and mechanically ventilated. Complete anesthesia and relaxation were maintained by propofol infusion (0.2 $mg \cdot kg^{-1} \cdot min^{-1}$) and by repetitive boluses of pentobarbital (15 mg/kg IV plus 5 $mg \cdot kg^{-1} \cdot 15\ min^{-1}$) and pancuronium (0.2 $mg \cdot kg^{-1} \cdot 15\ min^{-1}$). Through the right carotid artery, a 5F pigtail 12-pole multielectrode combination conductance-pressure catheter (Millar Instruments or CD-Leycom, Zoetermeer) was placed in the LV and connected to a dual-field conductance processor (Sigma 5DF, CD-Leycom). Adequate position of the electrodes was confirmed by examination of the segmental volume signals. The volume signal was calibrated with high-frequency harmonic 2D echocardiographic images (biplane Simpson's method).[16]

Study 1: Comparison With Invasive Indices of Systolic Chamber Function

Nine pigs (54±10 kg; range, 35 to 65 kg) underwent median sternotomy without the pericardium being opened, and the heart was cradled. A snare was placed around the inferior vena cava for preload manipulation. Animals were studied at baseline, during dobutamine (n=9; 1 to 10 $\mu g \cdot kg^{-1} \cdot min^{-1}$) and esmolol (n=4; 25 to 200 $\mu g \cdot kg^{-1} \cdot min^{-1}$) infusions, and after left main coronary microembolization of polystyrene microspheres (n=4; mean diameter, 45 μm; Polysciences).[17] Instead of using fixed pre-established doses, we titrated perfusions to obtain a broad range of maximal elastance (E_{max}) measured online during each experiment.

In each state, simultaneous CDMM images and signals were acquired during end-expiratory apnea, followed immediately by transient caval occlusion while invasive data storage was maintained. This acquisition process was repeated 3 times for each state, with periods of waiting for stabilization of >5 minutes. The average of Doppler-derived EIVPD measurements of the 3 consecutive beats recorded just before caval occlusion was compared with the pressure-volume relationship indices obtained during the preload reduction maneuver performed immediately thereafter.

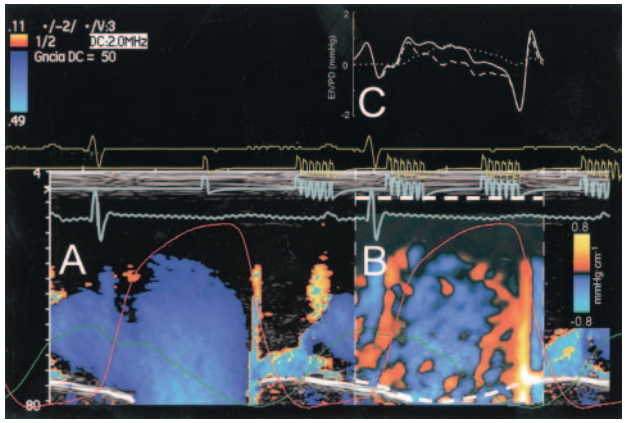

Figure 1. Example of image and signal acquisition and processing. Synchronicity, ECG (both in yellow), pressure (red), and volume (green) invasive signals are shown. A, Original CDMM image. B, Insertion of the pressure gradient map of the following beat. This color overlay displays the pressure difference between one pixel and another located 1 cm closer to the ultrasound probe (mm Hg/cm). Apical and LVOT positions for measuring EIVPDs are shown by thick white dashed lines. C, Total (solid line), inertial (dashed line), and convective (dotted line) components of the EIVPD for positions traced in B.

Study 2: Load Dependence

In 5 pigs, a small subxyphoid aperture was created in the abdominal wall to introduce the ultrasound probe, opening neither the peritoneum nor the thorax. This approach provides a suitable 5-chamber view in these animals. Occlusion balloons were placed in the inferior vena cava (right atrium junction) and in the descending thoracic aorta via the femoral vessels. Because the inotropic state may modify load dependence,[18] animals were studied at baseline and during infusion of dobutamine and esmolol (same dose range as study 1). For each inotropic steady state, CDMM and invasive data were simultaneously acquired immediately before and during 10 seconds of caval and aortic occlusion. Within each hemodynamic run, measurements of each individual beat recorded during balloon occlusion were compared with the average of 3 consecutive beats recorded at baseline. Data were obtained at end-expiration apnea without the ultrasound probe or the Doppler cursor being moved.

Echocardiographic Image Acquisition and Analysis

Broadband 2.0- to 4.0-MHz and 2.5- to 5-MHz transducers were used on a Sequoia C-256 system (Siemens AG). CDMM images were obtained from 5-chamber views as described.[13] The method used for digital image processing to obtain EIVPDs has been reported[12] and validated elsewhere.[13] Other authors have also demonstrated the accuracy of a similar approach to measure intraventricular pressure differences in diastole and its applicability in the clinical setting.[19,20] Briefly, if the M-mode cursor closely approximates a flow streamline, the spatiotemporal velocity distribution of a discrete blood sample is provided by the value of its corresponding pixel color: v(s,t), where v represents velocity, s represents the linear dimension of the streamline, and t is time. Thus, the color-Doppler M-mode recording provides the data necessary to solve Euler's momentum equation: $(\delta p/\delta s) = -\rho \cdot [(\delta v/\delta t) + v(\delta v/\delta s)]$, where p is pressure and ρ is blood density. The first and second terms on the right side of the equation account for inertial and convective acceleration, respectively. Once pressure gradient maps are obtained, total, inertial, and convective EIVPDs are calculated by spatial integration between the apex and the LVOT (Figure 1). Instead of a fixed distance between locations, these 2 positions are traced in each

image based on the grayscale layer and the pressure-gradient overlay. Peak and time to peak values of each of the 3 EIVPD curves were measured constrained to the ejection period, and all temporal values are reported with the QRS onset as reference. Intraobserver, interobserver, and beat-to-beat variabilities of EIVPD measurements (20 unselected patients referred for a conventional echocardiographic examination; independently and blindly acquired CDMM recordings) were 0.1±0.5 mm Hg (2±9%), 0.2±0.6 mm Hg (5±11%), and 0.1±0.7 mm Hg (2±12%), respectively.

Invasive Hemodynamic Measurements

All signals were digitized at 1000 Hz. By cross correlation of a synchronicity signal connected to the ultrasound scanner and the signal acquisition system, CDMM and invasive hemodynamic measurements were obtained for the same beat (Figure 1).[13]

Three indices of systolic function were derived from the pressure-volume loops obtained during caval occlusion: (1) E_{max}, defined as the slope of the end-systolic pressure-volume relationship;[3] (2) preload recruitable stroke work (PRSW), defined as the slope of the relationship between stroke work and end-diastolic volume (EDV);[21] and (3) the slope of the relationship between dP/dt_{max} and EDV (dP/dt_{max}/EDV).[22] The iterative linear regression method was used to calculate E_{max}.[23] Beats were selected after a 3- to 4-mm Hg decrease in end-systolic LV pressure, and a mean of 10 subsequent cycles was processed (6.5±3.0 seconds) to minimize the effect of autonomic reflexes. The end-systolic pressure-volume relationship was linear at all hemodynamic states (all $R>0.91$). Intraobserver, interobserver (10 randomly selected runs), and consecutive run-to-run (32 hemodynamic states) variabilities of E_{max} were 0.11±0.49, 0.23±0.51, and 0.14±0.37 mm Hg/mL, respectively.

Statistical Analysis

Linear mixed-effects (LME; S-Plus version 2000) models were used for analysis because repeated-measures designs were heavily unbalanced. Best linear unbiased estimators are reported for these models. Best linear unbiased estimators account for the mean expected values for fixed effects once the source of variation resulting from random effects is omitted. Significant LME models were followed by simulation contrasts.[24] For study 1, EIVPD was compared with E_{max}, PRSW, and dP/dt_{max}/EDV (fixed effects). For this purpose, 2 sets of models were calculated using a random animal effect, allowing either for different intercepts and slopes or only for different intercepts of regression lines within each animal. Within-animal correlation coefficients[25] and between-animals weighted regression models[26] were also computed. Pooled data obtained at baseline and during pharmacological interventions were categorized in 3 levels of systolic function based on E_{max} tertiles. Hemodynamic differences between categories (fixed effects) were then assessed by LME models (random animal effect) and all-pair contrasts. For study 2, the relative change from preocclusion values of EDV and peak systolic pressure was calculated for all occlusion beats and categorized in 5% intervals. Then, LME models were used to study the effects of the load percentage-change category (fixed effect) on the hemodynamic variables, nesting the hemodynamic run within the animal random effect. Simulation contrasts were calculated against baseline values. A value of $P<0.05$ was considered significant.

Scan Line Misalignment Error Analysis (Study 3)

The method used to estimate EIVPDs assumes that flow follows a linear streamline and that this streamline is coaxially interrogated to obtain the CDMM image. These assumptions may not always be met in clinical practice and can lead to significant bias, particularly because outflow is known to be skewed and axis asymmetric. Therefore, the potential error related to streamline linearization and nonoptimal scan line positioning was addressed in vivo. Using a biplane scanner (Philips Sonos 7500) and a matrix transducer, we acquired 36 color Doppler cine loops of LV outflow at end expiration every 5° in a healthy volunteer (see the expanded Methods section in the Data Supplement, found online at http://circ.ahajournals.org/cgi/content/full/CIRCULATIONAHA.104.485128/DC1). Loops were postprocessed to render a full 5D (3D+time+velocity) outflow data set.[27] The core position of the jet was calculated for all flow cross sections obtained in the long axis from the apex to the LVOT at peak flow rate.[28] The ideal scan line orientation was estimated as the biplane linear projection of this core position. Against the reference EIVPD calculated from this line, errors related to angle and parallel displacement were measured every 2.5° and 0.625 mm, respectively. Errors are reported as the mean±SD of the 360° spatial rotation at each misaligned position.

Results

Correlation of EIVPD With Invasive Indices of Systolic Function

A wide range of inotropic states were achieved (E_{max} range, 0.5 to 12.1 mm Hg/mL), and acute ischemic cardiomyopathy induced significant LV dilatation and depression of systolic function (Table 1). Peak EIVPD closely correlated with all invasive indices of systolic function (Table 2 and Figure 2). EIVPD was as sensitive as E_{max}, PRSW, and dP/dt_{max}/EDV in detecting differences between categories of systolic function (Table 1 and Figures 3 and 4). Within-animal and between-animals correlation coefficients of peak inertial EIVPD and invasive indices were $R=0.93$ and 0.94 for E_{max}, $R=0.81$ and 0.76 for PRSW, and $R=0.81$ and 0.87 for dP/dt_{max}/EDV ($P<0.001$ for all), respectively. Peak EIVPD was reached close to but slightly after ejection onset, whereas peak inertial EIVPD was achieved even closer to the onset (Table 1).

Load Dependence of EIVPDs

Caval occlusion remarkably decreased EDV and end-diastolic LV pressure without increasing heart rate (Table 3). Stroke volume, ejection fraction, and dP/dt_{max} significantly changed during preload manipulation. However, peak EIVPD remained constant. When EDV decreased >10%, peak inertial EIVPD increased by 15% to 23%. During aortic occlusion, peak LV pressure increased rapidly up to a relative change of 40%. Ejection fraction and stroke volume decreased, whereas dP/dt_{max} increased significantly (Table 4). Although nonsignificant, a trend toward a reduction of peak EIVPD at high afterload ($P=0.06$) was observed. Peak inertial EIVPD was unchanged by afterload interventions.

Scan Line Misalignment Error

The ejection jet core followed a predominantly linear trajectory in the frontal and sagittal planes of the LVOT (linear regression coefficients of their respective projections >0.9). Consequently, the error related to the linear trajectory assumption was only 0.15 mm Hg. The error in EIVPD resulting from scan line misalignment is represented in Figure 5. As shown, an angle misalignment of ±35° (in any spatial direction) was associated with an error of −0.2 to −0.6 mm Hg (95% confidence limits of agreement), whereas a ±0.5-cm coaxial displacement from centerline (representing a 50% uncertainty of the LVOT diameter size) induced an error of 0.3 to −0.7 mm Hg.

Discussion

The development of a strong noninvasive index of LV systolic function, comparable to the indices based on the pressure-volume relationship, has been a matter of several

TABLE 1. Hemodynamic Data Obtained at Baseline, During Pharmacological Interventions, and After Coronary Microembolization for Study 1

	LV Systolic Chamber Function				Acute Ischemic Cardiomyopathy		
	Low	Mid	High	SD	Baseline	Postembolization	SD
Animals, n	6	8	5	...	4	4	...
Data sets, n	32	33	33	...	10	10	...
Invasive							
Heart rate, bpm	90*†	101	112*	10	108	82‡	10
End-diastolic pressure, mm Hg	12	13	15	4	9	20‡	3
Peak systolic pressure, mm Hg	99*†	113	130*	15	111	81‡	10
End-diastolic volume, mL	52†	54	45*	7	55	64‡	7
End-systolic volume, mL	26†	23	21	5	22	40‡	7
Ejection fraction, %	51*†	56	57	7	62	39‡	5
dP/dt_{max}, mm Hg/s	1874*†	2815	4946*	995	2339	1239‡	293
Time to dP/dt_{max}, ms	56*†	45	33*	8	48	46	5
E_{max}, mm Hg/mL	1.5*†	3.2	7.6*	1.3	3.2	1.2‡	0.7
PRSW, mm Hg	38*†	62	82*	13	63	30‡	11
dP/dt_{max}/EDV, mm Hg · s^{-1} · mL^{-1}	12*†	51	110*	25	26	19	8
Doppler echocardiography							
Peak EIVPD, mm Hg	1.8*†	3.4	7.6*	1.5	3.4	1.1‡	0.8
Peak inertial EIVPD, mm Hg	1.3*†	2.4	4.9*	1.0	2.6	0.7‡	0.8
Peak convective EIVPD, mm Hg	0.8*†	1.9	4.2*	1.0	2.2	0.5‡	0.4
Ejection onset, ms	74*†	55	38*	16	55	60	11
Time to peak EIVPD, ms	102*†	75	59*	17	76	83	12
Time to peak inertial EIVPD, ms	97*†	70	54*	17	70	79‡	8
Time to peak convective EIVPD, ms	159*†	112	79*	26	100	119	16

SD is the within-group residual SD. Data represent the best linear unbiased estimators of the mean value within each LV systolic chamber function level adjusted for the animal random error.

*$P<0.05$ vs mid; †$P<0.05$ vs high; ‡$P<0.05$, postembolization vs baseline.

studies. Online measurements of LV areas using automatic border detection can provide an approximation to E_{max},[29] but this method requires an invasive measurement of pressure and acute preload interventions. Although tissue Doppler-derived myocardial acceleration[30] and systolic strain rate[16] have been recently correlated with E_{max}, the performance of these measurements as indicators of global LV function could be limited if regional wall motion is abnormal.

TABLE 2. Linear Regression Analysis of Peak EIVPD With Invasive Indexes of Systolic Chamber Function Based on the Pressure-Volume Relationship (Study 1)

Design	Intercept	Coefficient	*R*	*P*	Runs/Animals, n
E_{max}					
Within animal (random intercept and slope)	0.24	0.87	0.98	<0.001	104/9
Within animal (random intercept)	0.27	0.97	0.97	<0.001	104/9
Between animals	0.01	0.99	0.99	<0.001	9
PRSW					
Within animal (random intercept and slope)	21.41	10.78	0.91	<0.001	107/9
Within animal (random intercept)	36.17	7.27	0.81	<0.001	107/9
Between animals	25.96	7.96	0.86	0.003	9
dP/dt_{max}/EDV					
Within animal (random intercept and slope)	−8.72	16.40	0.91	<0.001	105/9
Within animal (random intercept)	−8.37	14.70	0.88	<0.001	105/9
Between animals	6.89	11.87	0.91	<0.001	9

Within-animal regression models account for the true correlation between indexes within each experimental animal, assuming either different or the same regression slopes for each animal.

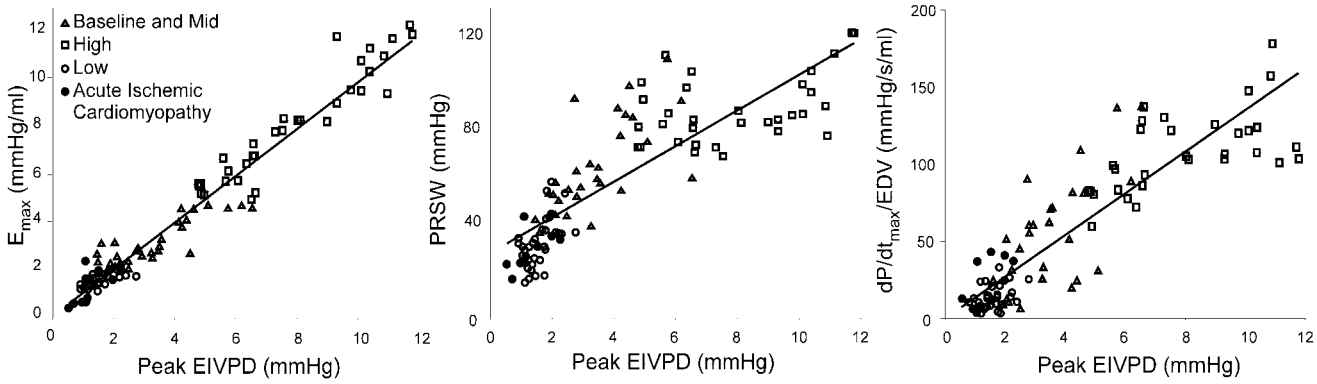

Figure 2. Correlation analysis of peak EIVPD and invasive indices of systolic function based on the pressure-volume relationship. Line represents the linear regression line fitted from pooled data from all animals.

Intraventricular Pressure Gradients and Systolic Function

Regional pressure gradients inside the LV take place during ejection in normal hearts. EIVPDs, the consequence of the resistance of intraventricular blood to inertial and convective acceleration, represent the force applied by the contracting ventricle per unit volume of accelerated blood.[5,6] The magnitude of EIVPDs has been shown to increase with exercise[8] and adrenergic stimulation[9] and to decrease with β-blocking agents in invasive studies.[7] Furthermore, peak EIVPD has shown a greater sensitivity and a more linear pattern than dP/dt_{max} for changes in the inotropic state in a computer fluid-dynamic simulation study.[11] Applying the same noninvasive method used in the present study, we have previously demonstrated that peak EIVPD is depressed in patients with dilated cardiomyopathy and is highly sensitive to inotropic drug interventions.[13]

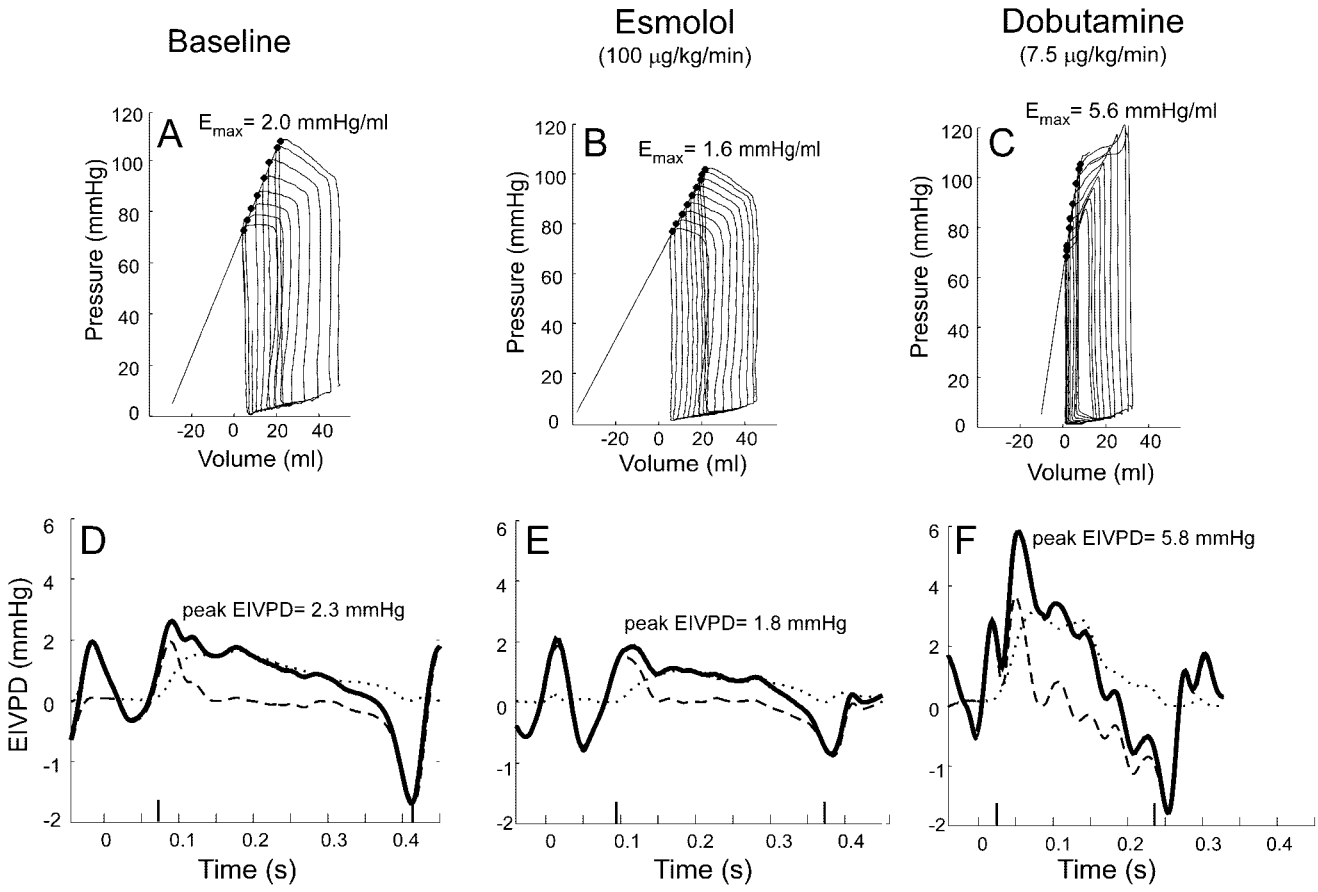

Figure 3. End-systolic pressure-volume relationship (A–C) and Doppler-derived EIVPD curves (D–F) at baseline (A, D) and during esmolol (B, E) and dobutamine (C, F) infusions in a representative study. EIVPDs represented as in Figure 1.

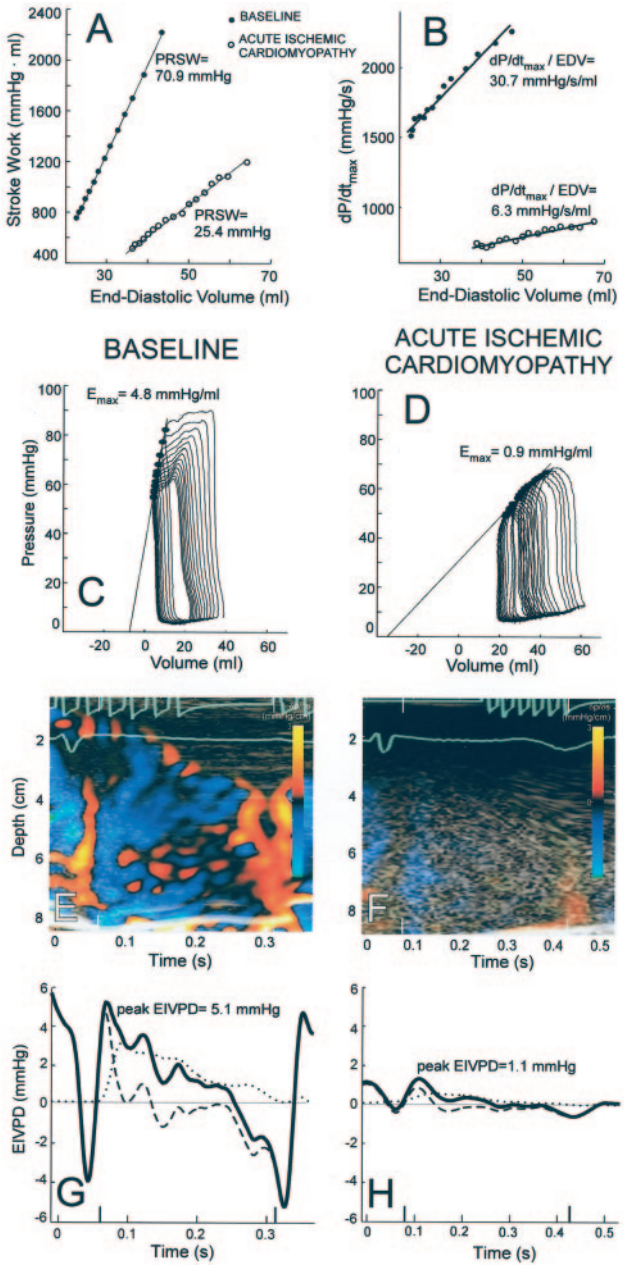

Figure 4. Values of PRSW (A), dP/dt_{max}/EDV (B), E_{max} (C, D), ejection intraventricular pressure gradient maps (E, F), and EIVPD curves (G, H) obtained at baseline and during acute ischemic cardiomyopathy in a representative animal. EIVPD components represented as in Figures 1 and 3.

Load Dependence

The nature of load dependence in vivo is often complex and nonlinear; thus, several indices can be significantly affected by preload and afterload yet can be relatively independent of load over a specified range.[15,18,31] Even methods based on the pressure-volume relationship can be slightly influenced by load in the intact circulation.[32] In our study, peak EIVPD showed to be relatively load independent. Importantly, the magnitude of the load interventions performed in our study was higher than those explored in previous studies assessing the stability of Doppler-derived indices of systolic function.[30,33]

A nearly significant trend toward partial afterload dependence of total EIVPD was found. Because of the competitiveness between intrinsic and extrinsic components of systolic load,[5] the intraventricular pressure drop increases when aortic pressure is reduced and vice versa. This interaction between afterload components is the manifestation of the inverse force-velocity relationship of contraction and has been demonstrated in situations of predominantly convective gradients such as aortic valve stenosis.[34] However, without outflow obstruction, EIVPDs are mediated mostly by inertial forces[5,13] and behave differently; as shown in the present study, inertial EIVPD is unaffected by afterload (Table 4). The fact that inertial EIVPD reaches its peak very early during ejection (Table 1) probably explains why this index is less afterload dependent than other ejection phase indices. Furthermore, the close correlation observed between inertial EIVPD and E_{max} conforms to the well-known relationship between flow acceleration and inotropic state.[11,33]

Clinical Implications

Ejection fraction is the pivotal index of systolic function in clinical practice. Although the clinical utility of ejection fraction is well established, this index may be unreliable because of inaccuracy in the estimation of LV volumes and, most importantly, its load dependence.[31] Ejection fraction is particularly modified by load when contractility is impaired,[18] an issue that limits its applicability under extreme or changing load conditions. In these situations, Doppler-derived EIVPDs could provide a more reliable measurement of systolic chamber function.

Because the Doppler signal is less sensitive to noise than cross-sectional echocardiography, EIVPDs are obtainable even in patients in whom poor endocardial definition precludes an accurate estimation of LV volumes. The present study demonstrates that the measurements of EIVPDs are relatively accurate as long as scan line misalignment is $<30°$ and displacement from the LVOT center is <0.5 mm. Because CDMM acquisition is always guided by 2D echocardiography, these constraints generally can be met during clinical examination, as suggested by our reproducibility results.

Study Limitations

The present study sought to characterize LV systolic function through the analysis of chamber pump parameters. Assessing myocardial function is a different issue that involves the analysis of aspects such as fiber strain and sarcomere length. To correlate indices of chamber function with true myocardial function, it needs to be assumed that instantaneous modifications of chamber volume directly follow changes in fiber length. However, in the presence of abnormal ventricular geometry, this may not always be the case. In fact, chamber dynamics are known to overestimate myocardial function when LV wall thickness is increased.[1] Therefore, the performance of EIVPDs in the presence of abnormal chamber geometry resulting from hypertrophy or regional wall motion abnormalities deserves further investigation. In addition, because the sizes of animals we used for our correlation study were relatively homogeneous, the

TABLE 3. Hemodynamic Data During Preload Reduction by Caval Occlusion (Study 2)

	Relative Change LV End-Diastolic Volume %										
	Pre-Occl	0–5	5–10	10–15	15–20	20–25	25–30	30–35	35–40	SD	*P*
Beats, n	26	43	43	24	23	22	20	20	16		
End-diastolic volume, mL	63	62	59*	55*	52*	49*	46*	42*	38*	2	<0.001
End-diastolic pressure, mm Hg	15	11*	7*	5*	3*	3*	2*	1*	1*	2	<0.001
dP/dt_{max}, mm Hg/s	2285	2304	2351	2382*	2347	2347	2277	2237	2203	110	<0.001
Peak systolic pressure, mm Hg	98	97	95*	92*	89*	85*	82*	81*	79*	3	<0.001
Ejection fraction, %	52	55	55	56	59*	61*	63*	64*	64*	5	<0.001
Stroke volume, mL	33	34	32	31*	31	30*	29*	28*	25*	3	<0.001
Heart rate, bpm	85	84	84	83	84	83	84	83	83	2	0.08
Peak EIVPD, mm Hg	4.3	4.4	4.5	4.6	4.6	4.6	4.6	4.5	4.3	0.4	0.11
Peak inertial EIVPD, mm Hg	2.6	2.8	2.8	2.9*	3*	3*	3.2*	3.1*	3.1*	0.4	<0.001
Peak convective EIVPD, mm Hg	3.2	3.2	3.1	3.1	3	3	2.6*	2.7*	2.3*	0.3	<0.001

Pre-Occl indicates baseline preocclusion values. Data represent the best linear unbiased estimators of fitted values within each load category adjusted for the hemodynamic run and animal random errors; probability value is the significance of the linear mixed-effects model.

*$P<0.05$ vs preocclusion.

value of EIVPDs in a wider range of LV volumes should be explored. In dilated ventricles, the greater disproportion between the LV chamber and the LVOT hypothetically could increase the convective component of EIVPD. However, we have previously shown that, in patients with dilated cardiomyopathy, reduced ejection velocities cause convective forces to be lower than in normal hearts; in fact, total EIVPDs are smaller.[13] Additionally, the small sample size used for studies 1 and 2 limits the precision of statistical estimates and reduces power to detect modest and moderate fixed effects.

For study 3, we used 3D color Doppler to obtain the volumetric data set, therefore constraining data acquisition to an axial interrogation of flow velocity. Phase-contrast cardiac magnetic resonance can provide the full 3D vectorial velocity information noninvasively but at a lower spatial, temporal, and velocity resolution than color Doppler. Although ignoring the other 2 velocity components could theoretically lead to underestimation of the true EIVPD, several pieces of evidence support that the error related to an axial interrogation of ejection flow is negligible. First, magnetic resonance studies have confirmed that ejection flow follows a mostly 1D trajectory without vorticity.[35] Second, although LV diastolic filling flow is known to also follow a slightly curvilinear trajectory,[35] a similar 1D simplification has been validated for LV filling.[19,20,36] Third, the excellent accuracy of Euler's equation for calculating EIVPDs would not stand if significant nonaxial components of flow velocity were present during ejection.[13] Another limitation of study 3 is that this type of reliability analyses is obviously model dependent. Consequently, misalignment errors could be higher in ventricles with geometrical variations such as localized septal hypertrophy. In situations like this one in which 2D color Doppler imaging shows that flow follows a tightly curved trajectory, magnetic resonance may be an alternative for measuring EIVPDs.[37]

TABLE 4. Hemodynamic Data During Afterload Manipulation by Aortic Occlusion (Study 2)

	Relative Change LV Peak Systolic Pressure, %										
	Pre-Occl	0–5	5–10	10–15	15–20	20–25	25–30	30–35	35–40	SD	*P*
Beats, n	30	55	21	23	16	38	51	29	11		
Peak systolic pressure, mm Hg	104	106	111*	118*	123*	129*	133*	137*	139*	3	<0.001
End-diastolic pressure, mm Hg	16	16	16	17	17	18*	18*	19*	19*	2	<0.001
dP/dt_{max}, mm Hg/s	2488	2524	2513	2445	2618*	2693*	2619*	2588	2527	133	<0.001
End-diastolic volume, mL	65	65	65	65	64	64	65	65	66	2	0.25
Ejection fraction, %	54	53	52*	49*	49*	48*	47*	46*	44*	2	<0.001
Stroke volume, mL	35	34	34	32*	32*	31*	31*	30*	29*	2	<0.001
Heart rate, bpm	87	87	88	83*	86	87	88	86	87	4	0.01
Peak EIVPD, mm Hg	4.2	4.1	4	4.2	3.9	3.9	3.7	3.5	3.7	0.8	0.06
Peak inertial EIVPD, mm Hg	2.5	2.4	2.5	2.5	2.6	2.6	2.4	2.3	2.3	0.6	0.6
Peak convective EIVPD, mm Hg	3	3	2.8	2.9	2.7	2.7	2.6*	2.5*	2.6	0.6	0.01

See Table 3 for explanation and abbreviations.

*$P<0.05$ vs preocclusion.

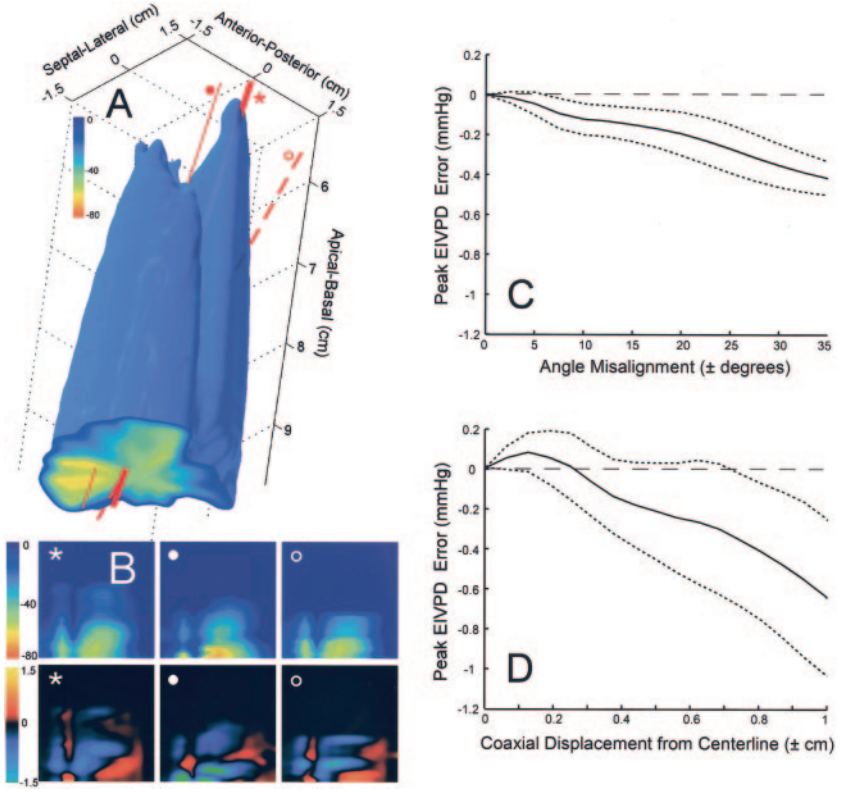

Figure 5. Scan line misalignment error analysis. A, Spatial distribution of ejection flow velocity at the instant of peak flow rate. At the LVOT level (cross section), velocities are skewed toward the septum and anterior wall. The thick line (*) shows the linearly approximated central core of the jet. Examples of misalignment are shown for a 0.5-cm coaxial displacement (thin line, ●) and a 30° angulation (dashed line, ○). B, Velocity (top) and pressure gradient (bottom) spatiotemporal distributions rendered for core and misalignment positions shown in A. C, D, Error of peak EIVPD as a function of angular misalignment (C) and coaxial displacement from centerline (D). For each misalignment position, values show the mean (solid lines)±SD (dotted lines) of the error measured for the full 360° rotation.

Conclusions

Doppler-derived EIVPDs provide quantitative, reproducible, noninvasive, and relatively load-independent indices of LV systolic chamber function that closely correlate with reference methods. This new method should improve the echocardiographic assessment of LV systolic chamber function in the clinical setting.

Acknowledgments

This work was supported by grants PI031220, BF03/00031 (to R. Yotti), and G03/185 Nodo-UNED (partial support to M.M. Desco) from the Fondo de Investigación Sanitaria, Instituto de Salud Carlos III, Spain, and by a grant from the Sociedad Española de Cardiología. We are indebted to all personnel in the Unit of Experimental Medicine and Surgery from the Hospital General Universitario Gregorio Marañón for their assistance.

References

1. Shimizu G, Hirota Y, Kita Y, Kawamura K, Saito T, Gaasch WH. Left ventricular midwall mechanics in systemic arterial hypertension: myocardial function is depressed in pressure-overload hypertrophy. *Circulation.* 1991;83:1676–1684.
2. Suga H, Sagawa K, Shoukas AA. Load independence of the instantaneous pressure-volume ratio of the canine left ventricle and effects of epinephrine and heart rate on the ratio. *Circ Res*. 1973;32:314–322.
3. Sagawa K, Suga H, Shoukas AA, Bakalar KM. End-systolic pressure/volume ratio: a new index of ventricular contractility. *Am J Cardiol*. 1977;40:748–753.
4. Laszt L, Muller A. Uber den Druckverlauf im linken Ventrikel und Vorhof und in der Aorta ascendens. *Helv Physiol Pharmacol Acta*. 1951; 9:55–73.
5. Pasipoularides A. Clinical assessment of ventricular ejection dynamics with and without outflow obstruction. *J Am Coll Cardiol*. 1990;15: 859–882.
6. Isaaz K, Pasipoularides A. Noninvasive assessment of intrinsic ventricular load dynamics in dilated cardiomyopathy. *J Am Coll Cardiol*. 1991; 17:112–121.
7. Falsetti HL, Verani MS, Chen CJ, Cramer JA. Regional pressure differences in the left ventricle. *Cathet Cardiovasc Diagn*. 1980;6:123–134.
8. Pasipoularides A, Murgo JP, Miller JW, Craig WE. Nonobstructive left ventricular ejection pressure gradients in man. *Circ Res*. 1987;61: 220–227.
9. Butler CK, Wong AY, Armour JA. Systolic pressure gradients between the wall of the left ventricle, the left ventricular chamber, and the aorta during positive inotropic states: implications for left ventricular efficiency. *Can J Physiol Pharmacol*. 1988;66:873–879.
10. Rushmer R. Initial ventricular impulse: a potential key to cardiac evaluation. *Circulation*. 1964;29:268–283.
11. Redaelli A, Montevecchi FM. Intraventricular pressure drop and aortic blood acceleration as indices of cardiac inotropy: a comparison with the first derivative of aortic pressure based on computer fluid dynamics. *Med Eng Phys*. 1998;20:231–241.
12. Bermejo J, Antoranz JC, Yotti R, Moreno M, Garcia-Fernandez MA. Spatio-temporal mapping of intracardiac pressure gradients: a solution to Euler's equation from digital postprocessing of color Doppler M-mode echocardiograms. *Ultrasound Med Biol*. 2001;27:621–630.
13. Yotti R, Bermejo J, Antoranz JC, Rojo-Alvarez JL, Allue C, Silva J, Desco MM, Moreno M, Garcia-Fernandez MA. Noninvasive assessment of ejection intraventricular pressure gradients. *J Am Coll Cardiol*. 2004; 43:1654–1662.
14. Matre K, Kvitting P, Zhou YQ, Faerestrand S. The effect of body weight on the degree of blood velocity profile skewness in the aortic annulus in domestic pigs. *Lab Anim*. 2003;37:72–80.
15. Mahler F, Ross JJ, O'Rourke RA, Covell JW. Effects of changes in preload, afterload and inotropic state on ejection and isovolumic phase measures of contractility in the conscious dog. *Am J Cardiol*. 1975;35: 626–634.
16. Greenberg NL, Firstenberg MS, Castro PL, Main M, Travaglini A, Odabashian JA, Drinko JK, Rodriguez LL, Thomas JD, Garcia MJ. Doppler-derived myocardial systolic strain rate is a strong index of left ventricular contractility. *Circulation*. 2002;105:99–105.
17. Smiseth OA, Mjos OD. A reproducible and stable model of acute ischaemic left ventricular failure in dogs. *Clin Physiol*. 1982;2:225–239.
18. Kass DA, Maughan WL, Guo ZM, Kono A, Sunagawa K, Sagawa K. Comparative influence of load versus inotropic states on indexes of ventricular contractility: experimental and theoretical analysis based on pressure-volume relationships. *Circulation*. 1987;76:1422–1436.

19. Greenberg NL, Vandervoort PM, Firstenberg MS, Garcia MJ, Thomas JD. Estimation of diastolic intraventricular pressure gradients by Doppler M-mode echocardiography. *Am J Physiol*. 2001;280:H2507–H2515.
20. Rovner A, Smith R, Greenberg NL, Tuzcu EM, Smedira N, Lever HM, Thomas JD, Garcia MJ. Improvement in diastolic intraventricular pressure gradients in patients with HOCM after ethanol septal reduction. *Am J Physiol*. 2003;285:H2492–H2499.
21. Glower DD, Spratt JA, Snow ND, Kabas JS, Davis JW, Olsen CO, Tyson GS, Sabiston DC Jr, Rankin JS. Linearity of the Frank-Starling relationship in the intact heart: the concept of preload recruitable stroke work. *Circulation*. 1985;71:994–1009.
22. Little WC. The left ventricular dP/dtmax–end-diastolic volume relation in closed-chest dogs. *Circ Res*. 1985;56:808–815.
23. Kono A, Maughan WL, Sunagawa K, Hamilton K, Sagawa K, Weisfeldt ML. The use of left ventricular end-ejection pressure and peak pressure in the estimation of the end-systolic pressure-volume relationship. *Circulation*. 1984;70:1057–1065.
24. Edwards D, Berry JJ. The efficiency of simulation-based multiple comparisons. *Biometrics*. 1987;43:913–928.
25. Bland JM, Altman DG. Calculating correlation coefficients with repeated observations, part 1: correlation within subjects. *BMJ*. 1995;310:446.
26. Bland JM, Altman DG. Calculating correlation coefficients with repeated observations, part 2: correlation between subjects. *BMJ*. 1995;310:633.
27. Bermejo J, Lang RM, Odreman R, Mulet M, Saunders J, Weinert L, Sugeng L, Moreno M, Garcia Fernandez MA. Four-dimensional surface-tracking of contrast-enhanced transthoracic biplane echocardiograms: a new tool for quantitative assessment of LV function. *J Am Coll Cardiol.* 2003;41:437A. Abstract.
28. Tsujino H, Jones M, Shiota T, Qin JX, Greenberg NL, Cardon LA, Morehead AJ, Zetts AD, Travaglini A, Bauer F, Panza JA, Thomas JD. Real-time three-dimensional color Doppler echocardiography for characterizing the spatial velocity distribution and quantifying the peak flow rate in the left ventricular outflow tract. *Ultrasound Med Biol*. 2001;27:69–74.
29. Gorcsan J, III, Denault A, Mandarino WA, Pinsky MR. Left ventricular pressure-volume relations with transesophageal echocardiographic automated border detection: comparison with conductance-catheter technique. *Am Heart J*. 1996;131:544–552.
30. Vogel M, Cheung MM, Li J, Kristiansen SB, Schmidt MR, White PA, Sorensen K, Redington AN. Noninvasive assessment of left ventricular force-frequency relationships using tissue Doppler-derived isovolumic acceleration: validation in an animal model. *Circulation*. 2003;107:1647–1652.
31. Quinones MA, Gaasch WH, Alexander JK. Influence of acute changes in preload, afterload, contractile state and heart rate on ejection and isovolumic indices of myocardial contractility in man. *Circulation*. 1976;53:293–302.
32. Baan J, Van der Velde ET. Sensitivity of left ventricular end-systolic pressure-volume relation to type of loading intervention in dogs. *Circ Res*. 1988;62:1247–1258.
33. Bauer F, Jones M, Shiota T, Firstenberg MS, Qin JX, Tsujino H, Kim YJ, Sitges M, Cardon LA, Zetts AD, Thomas JD. Left ventricular outflow tract mean systolic acceleration as a surrogate for the slope of the left ventricular end-systolic pressure-volume relationship. *J Am Coll Cardiol*. 2002;40:1320–1327.
34. Bermejo J, Rojo-Alvarez JL, Antoranz JC, Abel M, Burwash IG, Yotti R, Moreno M, Garcia-Fernandez MA, Lehmann KG, Otto CM. Estimation of the end of ejection in aortic stenosis: an unreported source of error in the invasive assessment of severity. *Circulation*. 2004;110:1114–1120.
35. Kilner PJ, Yang GZ, Wilkes AJ, Mohiaddin RH, Firmin DN, Yacoub MH. Asymmetric redirection of flow through the heart. *Nature*. 2000;404:759–761.
36. Greenberg NL, Krucinski S, Thomas JD. Significance of color Doppler M-mode scanline orientation in the non-invasive assessment of intraventricular pressure gradients. In: *Computers in Cardiology*. Piscataway, NJ: IEEE Press; 1997:605–608.
37. Thompson RB, McVeigh ER. Fast measurement of intracardiac pressure differences with 2D breath-hold phase-contrast MRI. *Magn Reson Med*. 2003;49:1056–1066.

CLINICAL PERSPECTIVE

Ejection intraventricular pressure gradients are related to the inotropic state of the left ventricle. Thus, their measurement may be useful for quantifying systolic function. In the absence of an anatomic obstruction, intracardiac pressure gradients cannot be estimated from the simplified Bernoulli equation. However, we have developed and validated a method for measuring the ejection intraventricular pressure difference (EIVPD) between the apex and outflow tract by postprocessing color Doppler M-mode images. The present study demonstrates, in a high-fidelity instrumentation animal setup, that Doppler-derived EIVPDs correlate closely with reference indices of systolic chamber function based on the pressure-volume relationship. The study also shows that EIVPDs are reproducible and relatively unaffected by ventricular load. In the clinical setting, ejection fraction is the pivotal index of systolic function, but its reliability is frequently limited by technical limitations and load dependence. Hypothetically, under extreme or changing load conditions (ie, regurgitant valve disease), Doppler-derived EIVPDs could provide a more accurate measurement of systolic function. In addition, the robustness of EIVPDs suggests a potential value for quantifying myocardial reserve and assessing the response to pharmacological, surgical, and resynchronization therapies. Color Doppler M-mode images are easy to obtain during a standard echo Doppler examination, and the mathematical algorithms to measure EIVPDs can be readily incorporated into the software of ultrasound scanners. Therefore, this new method may improve the assessment of left ventricular systolic function with echocardiography, particularly in situations in which a quantitative measurement is mandatory to guide therapy.